applied nano

MDPI

Article

Characterization of Organic Molecules Grafted to Silica or Bismuth Nanoparticles by NMR

Céline Henoumont [1], Gauthier Hallot [2], Estelle Lipani [1], Catherine Gomez [2], Robert N. Muller [1,3], Luce Vander Elst [1], Marc Port [2] and Sophie Laurent [1,3,*]

[1] General, Organic and Biomedical Chemistry Unit, NMR and Molecular Imaging Laboratory, University of Mons, 19 Avenue Maistriau, 7000 Mons, Belgium; Celine.HENOUMONT@umons.ac.be (C.H.); Estelle.Lipani@umons.ac.be (E.L.); Robert.Muller@umons.ac.be (R.N.M.); luce.vanderelst@umons.ac.be (L.V.E.)

[2] Laboratoire de Génomique, Bioinformatique et Chimie Moléculaire (EA 7528), Equipe Chimie Moléculaire, Conservatoire National des Arts et Métiers (Cnam), HESAM Université, 2 Rue Conté, 75003 Paris, France; gauthier.hallot@nexdot.fr (G.H.); catherine.gomez@lecnam.net (C.G.); marc.port@lecnam.net (M.P.)

[3] Center for Microscopy and Molecular Imaging (CMMI), 8 Rue Adrienne Boland, 6041 Gosselies, Belgium

* Correspondence: sophie.laurent@umons.ac.be; Tel.: +32-65-373525

Abstract: NMR is a powerful characterization tool and we propose to study the surface of silica or bismuth nanoparticles dedicated to medical applications in order to evidence the covalent grafting of organic molecules on their surface. For that aim, DOSY experiments are particularly useful and allow for the discrimination of molecules interacting strongly with the nanoparticle surface from molecules simply weakly adsorbed at the surface. We were able to characterize thoroughly the surface of different silica and bismuth nanoparticles.

Keywords: nanoparticles surface; DOSY; NMR

check for updates

Citation: Henoumont, C.; Hallot, G.; Lipani, E.; Gomez, C.; Muller, R.N.; Vander Elst, L.; Port, M.; Laurent, S. Characterization of Organic Molecules Grafted to Silica or Bismuth Nanoparticles by NMR. *Appl. Nano* **2021**, 2, 330–343. https://doi.org/10.3390/applnano2040024

Academic Editor: Angelo Maria Taglietti

Received: 29 June 2021
Accepted: 15 October 2021
Published: 4 November 2021

Publisher's Note: MDPI stays neutral with regard to jurisdictional claims in published maps and institutional affiliations.

Copyright: © 2021 by the authors. Licensee MDPI, Basel, Switzerland. This article is an open access article distributed under the terms and conditions of the Creative Commons Attribution (CC BY) license (https://creativecommons.org/licenses/by/4.0/).

1. Introduction

Nanoparticles (NP) are more and more explored for applications in the medical field. They can be used as drug delivery systems but also as contrast agents for different imaging techniques. We can cite silica-based nanoparticles, liposomes, polymersomes or inorganic NP such as iron oxide NP, gold NP, silver based NP, zinc oxide NP, bismuth NP, quantum dots, etc. [1]. An important issue for the use of NP in the medical field is to be able to derivatize the surface in order to obtain stable suspensions in aqueous media and buffer and also to vectorize the NP for targeting, meaning that we have to possess robust tools to characterize their surface, and more precisely, to attest of the covalent grafting of the ligands of interest to their surface.

Nuclear Magnetic Resonance (NMR) is a powerful tool to determine if an organic ligand is covalently attached to a nanoparticle or if it is, on the contrary, simply adsorbed at the surface of the nanoparticle, with an exchange taking place between the free and the bound form of the ligand. Indeed, in addition to the classical 1D and 2D NMR spectra, diffusion ordered spectroscopy (DOSY) experiments are particularly useful for these type of investigations [2–4]. It allows the determination of the diffusion coefficients of the solution species and will thus allow to discriminate between covalently grafted ligands and adsorbed ligands. Indeed, if the ligand is covalently attached to the nanoparticle, its diffusion coefficient will be equal to that of the nanoparticle. On the contrary, if the ligand is simply adsorbed on the nanoparticle surface, an average diffusion coefficient between those of the free and of the bound ligand should be observed because of the fast exchange between these two species (Equation (1)).

$$D_{obs} = P_B D_B + (1 - P_B) D_F \quad (1)$$

where D_B and D_F are the diffusion coefficients of the bound and of the free ligands respectively, and P_B is the molar proportion of the bound ligand.

In this work, we propose to demonstrate the power of the NMR tools to characterize the NP surface on two different types of NP. The first type, silica NP, could be useful in the context of magnetic resonance imaging (MRI), which is now a well-established technique in the medical field. MRI allows one to obtain, non-invasively, morphological and functional images in order to investigate the anatomy and physiology of the body, both in healthy and diseased conditions. MRI images can be obtained without the use of contrast agents, but some diagnostic questions cannot be elucidated easily and require the use of contrast agents. Even if other types of contrastophores, like CEST (chemical exchange saturation transfer) agents [5–7] start to emerge, two main classes of contrast agents can still be distinguished [8,9]: the paramagnetic contrast agents, which are mainly composed of gadolinium complexes [10–12], and the superparamagnetic ones, which are made of iron oxide NP [13,14]. They are respectively responsible for a brightening and of a darkening of the image area where they are accumulated, and are therefore respectively considered as positive and negative contrast agents.

Currently, the paramagnetic contrast agents are always preferred by the radiologists because a brightening of the diseased image area is more easy to visualize. Gadolinium complexes suffer, however, from a relatively low relaxivity (The relaxivity of a contrast agent is the increase of the water proton relaxation rate induced by 1 mmole per liter of the contrastophore.), which reflects the efficacy of the contrast agent. Many efforts are thus produced in the literature to improve it [15–17]. An elegant method to achieve this goal is to graft several small gadolinium complexes on a macromolecular object. The benefit is indeed double: first the grafting of a gadolinium complex on a bigger entity will increase its relaxivity thanks to the increase of its rotational correlation time; and secondly the presence of several gadolinium chelates on the same macromolecular object increases the efficacy of the whole entity [15–17]. Several macromolecular objects can be envisaged, like proteins [18,19], liposomes or micelles [20,21], dendrimers [22,23], polymers [24,25], or nanoparticles [26,27], such as silica nanoparticles [28]. They indeed possess several advantages: they are low cost, stable, safe, biocompatible, and endowed with a high water dispersibility. Moreover, their synthesis is quite easy and allows for the tuning of the particle size, which is important for applications in the biomedical field. As the covalent grafting of the gadolinium chelates at the nanoparticle surface is the key to obtain a high efficacy of the entity, the characterization of this binding is of crucial importance and we propose to describe an NMR method allowing this investigation.

The second NP studied in this work are metallic bismuth NP which possess the same advantages as silica NP in terms of low cost and biocompatibility and could have interesting applications in the medical field as a radiosensitizer in the context of radiotherapy [29–32], or as contrast agents in X-ray imaging thanks to the high atomic number of bismuth [33–36]. A few studies are nevertheless available on those NP [37] and a first challenge is to be able to synthesize stable aqueous suspensions by coating the NP with organic molecules. Two different ligands were used in that aim: the citrate ligand, which could interact with the surface thanks to its carboxylate functions, and the lipoic acid ligand modified with PEG, bearing thiol groups to interact with the NP surface. Again, NMR and more particularly DOSY experiments [38] will be used to evaluate the best ligand to stabilize the bismuth NP, which is also important to ensure a high NP stability in biological media and avoid harmful aggregation.

2. Materials and Methods

Chemicals: *N*-(3-dimethylaminopropyl)-*N′*-ethyl-carbodiimide hydrochloride (EDCI) and *O*-(2-aminoethyl)-*O′*-methylpolyethylene glycol of 750 g/mol molecular weight (PEG) were purchased from Sigma-Aldrich (Diegem, Belgium). 2-(4-aminobenzyl)diethylenetriaminepentaacetic acid (p-NH_2-Bn-DTPA) was furnished by Macrocyclics (Dallas, TX, USA) and was complexed with lanthanum ion from the lanthanum chloride salt ($LaCl_3$) at pH 6.5

in deionized water during 24 h [28]. Bismuth citrate sodium (Alfa Aesar, >94%), D-glucose (Sigma, 99.5%), citric acid (Labosi, >98%), lipoic acid (TCI, >97%), methylpolyethylene glycol of 750 g/mol molecular weight (PEG) (Alfa Aesar) were used without further purification. All solutions were prepared using fresh, distillated H_2O.

Synthesis of the silica nanoparticles and coupling reaction: The silica NP were synthesized as described in [28]. Briefly, a conventional water-in-oil microemulsion (8 mL of cyclohexane, 2 mL of hexanol, 2 mL of Triton X-100 and 1 mL of deionized water) was used. 100 µL of TEOS (tetraethoxysilane) and 60 µL of NH_4OH were then added and mixed during 24 h, followed by the addition of 50 µL of TEOS and 50 µL of CETS (carboxyethylsilanetriol) and an additional stirring of 24 h. The NPs are finally precipitated with 20 mL of acetone and washed with ethanol before being dispersed in deionized water. As they are made from TEOS and CETS, they possess carboxylate groups on their surface in order to allow the covalent grafting of different organic molecules. The number of those carboxylate functions were estimated to be about 2.4 carboxylate groups per nm^2 by conductimetric analyses (data not shown). The lanthanum complex, La-p-NH_2-Bn-DTPA, and PEG, having a terminal amine group, were grafted on the silica NP via an amide bond by using the coupling agent EDCI [28]. A five times excess of those molecules was used compared to the number of carboxylate groups. When both molecules are grafted at the nanoparticle surface, the La-complex was first grafted followed by PEG. The coupling reaction was tested at two different times (4 h and 24 h), and the NMR study was performed in order to evaluate the most appropriate coupling reaction time to obtain a covalent grafting. The purification of the reaction mixture was performed by ultracentrifugation on centrifugal filter units with a 10k cut-off (Amicon Ultra-15 10K device, Millipore, Brussels, Belgium). The NPs were characterized by DLS measurements before and after the grafting reactions and a quite similar measured diameter of about 35 nm was obtained.

Synthesis of metallic bismuth nanoparticles and coating exchange: Metallic bismuth NP were synthesized from an aqueous bismuth citrate solution. Citric acid and D-glucose, dissolved in distilled water, were then added to the previous solution. The pH was adjusted to reach a pH of 13 with a NaOH solution. The solution was heated in a continuous flow device controlled by a HPLC pump [39] and then cooled at room temperature. Finally, the crude was purified by ultrafiltration (filtration membrane of 30 kDa, Merck KGaA, Darmstadt, Germany). After washing with water at pH = 7, the purified bismuth NP dispersed in water were analyzed by NMR.

A ligand exchange procedure was used to modify the bismuth NP surface. For that purpose, a lipoic acid derivative (AL-PEG_{750}-OMe) was added to an aqueous solution of nanoparticles at pH = 7 and the solution was stirred at room temperature for 24 h. Subsequently, the metallic bismuth NP coated by AL-PEG_{750}-OMe were purified by ultrafiltration on a 30 kDa filter (Merck®) and washed with water at pH = 7 prior to NMR analysis. The NPs were characterized by DLS measurements and a diameter of about 65 nm was obtained.

NMR measurements: All the measurements were performed with a traditional 5 mm probe at 500 MHz on an AvanceII 500 spectrometer (Bruker, Karlsruhe, Germany). All the aqueous silica nanoparticle suspensions were diluted with D_2O to obtain 10% of D_2O. The 1D spectra were recorded with the noesypr1d sequence, allowing the suppression of the water peak with 64 scans. All the spectra were recorded with a relaxation delay of 3 s, except the spectra dedicated to the quantification of the grafted organic molecules, which were recorded with a longer relaxation delay of 100 s. These spectra allowing the quantification were recorded with an external reference of known concentration (TSP, 3-(trimethylsilyl) propionic-2,2,3,3-d_4 acid sodium salt, Sigma-Aldrich). 2D COSY NMR spectra were also recorded on some of the silica nanoparticle solutions, with 16 scans and 128 t_1 increments. For the measurements according to the pH, the pH was gradually increased with a NaOD solution and the pH was measured with a Mettler-Toledo pHmeter.

DOSY experiments were performed with the classical BPP-LED pulse sequence, which uses bipolar gradient pulses with two spoil gradients to measure the diffusion coefficients. A gradient pulse duration δ of 2 ms was used for all the experiments, with a diffusion delay Δ of 250 ms or 600 ms. 16 gradients incremented from 2% to 95% of the maximum gradient strength (53.5 G/cm) in a linear ramp were used, with a number of scans varying between 600 and 800 for each gradient value. The temperature was fixed at 298K. The raw data were extracted from the DOSY experiments and the observed decrease of the signal intensity with the gradient strength was fitted with the well-known diffusion equation (Equation (2)) [40,41]:

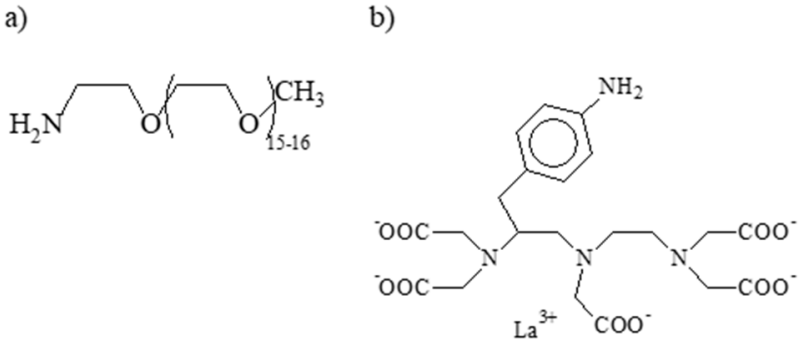
$$I = I_0 \exp[-\gamma^2 g^2 D \delta^2 (\Delta - (\delta/3) - (\tau/2))] \quad (2)$$

where I_0 is the intensity at 0% gradient, γ is the gyromagnetic ratio, g is the gradient strength, D is the diffusion coefficient, δ is the gradient pulse length, Δ is the diffusion time and τ is the interpulse spacing in the BPP-LED pulse sequence.

3. Results

3.1. Silica Nanoparticles

For this study, the silica NP were synthesized so that their surface was covered with carboxylate functions, which can be used to graft small ligands such as paramagnetic gadolinium complexes [28]. Two types of NP were studied: first, NP grafted with a small polyethylene glycol (PEG) having a molecular weight of 750 g/mol (needed in order to avoid a non-specific capture by the reticulo-endothelial system), and, secondly, NP grafted with PEG and with a diamagnetic analogue of a gadolinium complex, the Gd-*p*-NH_2-Bn-DTPA [28] (Scheme 1). This gadolinium complex, a derivative from the well-known Gd-DTPA, was substituted in the C4 position by an aminobenzyl group allowing its covalent grafting on the NP surface. However, with the gadolinium ion being paramagnetic, it prevents any NMR study because of a marked broadening of the different NMR peaks. A diamagnetic analogue is thus necessary and the lanthanum complex was used in this case.



Scheme 1. (**a**) Structure of the grafted polyethylene glycol. (**b**) Structure of La_*p*-NH_2_Bn_DTPA, the lanthanum complex which was grafted on the silica NP.

As mentioned in the introduction, the covalent grafting of the ligands was evaluated by NMR and two reaction times for the coupling reaction between the ligand and the NP surface was studied.

3.1.1. NMR Analysis of the Silica Nanoparticles Grafted with PEG and Synthesized with a Reaction Time of 4 h

The 1D NMR spectrum of the silica NP is presented at Figure 1 with, for comparison, the NMR spectra of PEG and of the bare NP bearing carboxylate functions on their surface. Several peaks can be distinguished on this 1D spectrum: the three characteristic peaks of PEG are clearly visible, as well as the two peaks coming from the carboxyethylsilanetriol (CETS), which is used during the synthesis to provide the carboxylate functions on the

nanoparticle surface. In addition to these peaks, additional signals coming from EDCI, used during the grafting synthesis as the coupling agent, and from ethanol, used to wash the NP after the synthesis, are also visible. The presence of these peaks is the evidence of an insufficient purification of the nanoparticle suspension after the synthesis, despite of the ultracentrifugation which was performed after the grafting reaction. It thus also means that the observed PEG is perhaps not completely covalently grafted on the nanoparticle surface but is partly free in solution because of the insufficient purification of the reaction mixture. It is thus very important to verify the covalent grafting of PEG on the nanoparticle surface, and for that, NMR provides several tools.

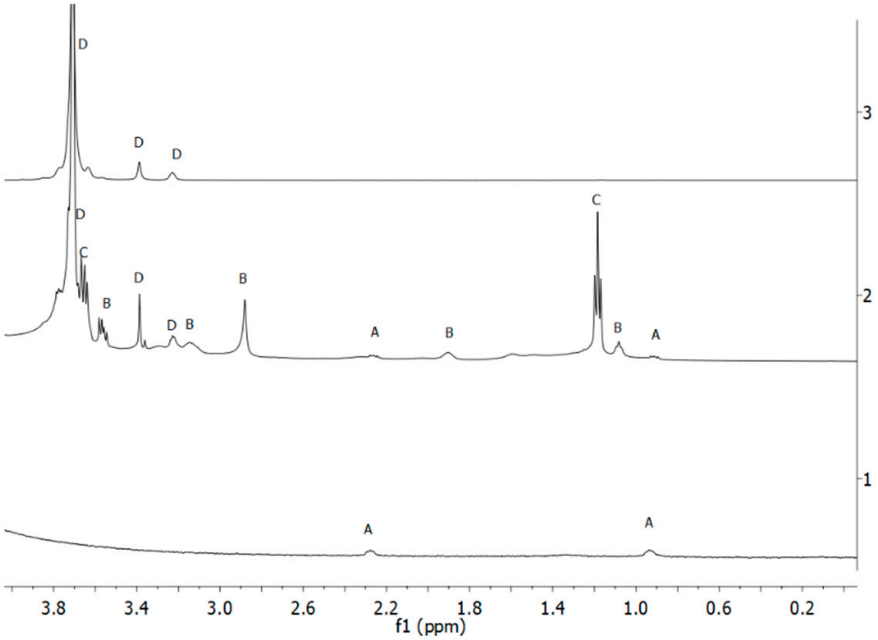


Figure 1. 1D NMR spectra recorded with the noesypr1d sequence on water suspensions prepared with 10% D_2O of the bare NP, bearing carboxylate functions on their surface (bottom spectrum), of the NP grafted with PEG (central spectrum), and of free PEG (top spectrum). The letters are used to assign the different peaks to the different molecules: A corresponds to CETS, B corresponds to EDCI, C corresponds to ethanol and D corresponds to PEG.

Firstly, NMR spectra of the NP suspensions were recorded at different pH (Figure 2). Indeed, as it was shown in [4], the peak at 3.20 ppm corresponding to the CH_2 near the amine group in free PEG is shifting with pH due to the protonation/deprotonation equilibrium of the amine group. But upon grafting, as the amine group is changed into an amide group, this shifting with pH should disappear. Nevertheless, what can be observed on Figure 3 is an important shift of this peak from 3.2 ppm at pH 6 to 2.75 ppm at pH 12. COSY spectra recorded at each pH allows the confirming of the belonging of these peaks to PEG (Figure S1). As it is exactly the behaviour observed for free PEG [4], this first study allows thus to conclude that most of the present PEG is free in solution. It does, nevertheless, not prevent some PEG covalently grafted to the silica NP from also being present, the peak corresponding to the CH_2 near the amide group being too small or too broad to be detected. A more robust tool to study the covalent coupling of organic molecules on NP is thus needed and, as described in the introduction, the use of DOSY experiments is very appropriate.

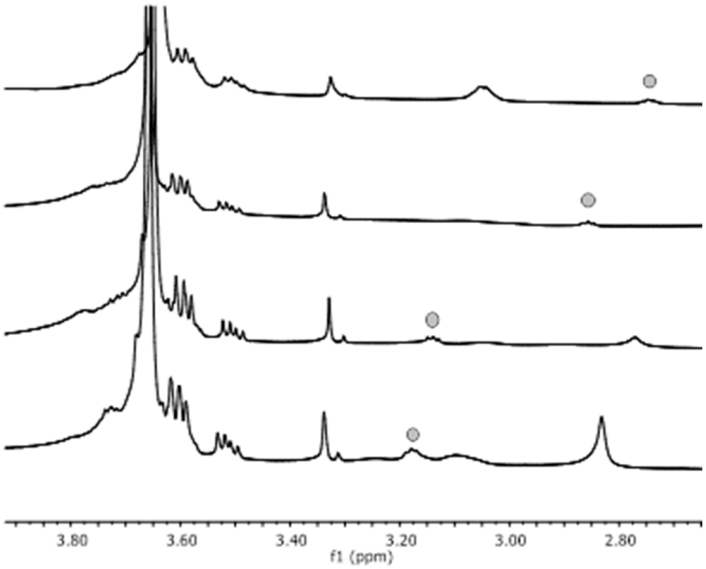


Figure 2. 1D NMR spectra recorded with the sequence noesypr1d on water suspensions prepared with 10% D_2O of the silica NP grafted with PEG at different pH: from the bottom to the top, the pH is equal to 6, 9, 10.5 and 12.

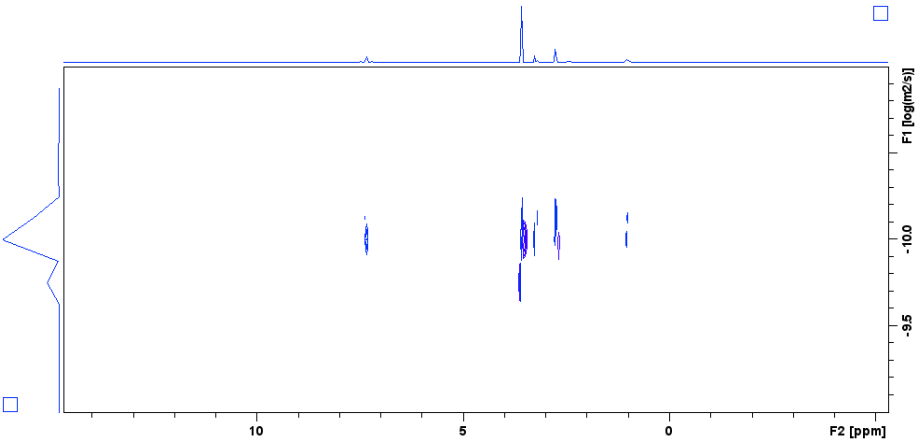


Figure 3. DOSY NMR spectrum recorded on silica NP grafted with PEG and the La-complex. The diffusion time Δ was set at 600 ms.

DOSY spectra were also recorded at different pH and the extracted diffusion coefficients of PEG are nearly equal to that of free PEG (Table 1), which tends to prove that PEG is mostly ungrafted on the NP surface and is simply adsorbed by an ionic interaction. A small increase of the diffusion coefficient of PEG with pH can be observed, which can be explained by a less efficient adsorption of PEG on the NP surface when the pH is increasing since the amine function of PEG becomes unprotonated and so uncharged. Nevertheless, a DOSY spectrum recorded at pH 7 with a longer diffusion time favouring slowly diffusing species (600 ms compared to 250 ms for the other DOSY spectra) allows for the extraction of diffusion curves with a biexponential decrease for nearly all the peaks of PEG. These biexponential curves can be fitted with one diffusion coefficient characteristic of free PEG ($D = 3.1 \times 10^{-10}$ m^2/s) and one characteristic of PEG grafted at the nanoparticle surface ($D = 1.6 \times 10^{-11}$ m^2/s). The relative intensities associated to these two diffusion coefficients allow for the estimation of a small grafting percentage of nearly 2% (Table 1 and Figure S2). It has to be noticed that for the peak corresponding to the methylene group next to the amine function, the extracted diffusion curve is monoexponential, with a diffusion coefficient which is that of free PEG (Figure S2). This can be explained by the fact that the

corresponding peak of the small amount of grafted PEG is at a different chemical shift and is probably too broad and too less intense to be detected.

Table 1. Extracted diffusion coefficients of PEG.

Δ = 250 ms		**Δ = 600 ms**	
SiO_2-PEG	**D ($\times 10^{-10}$ m^2/s)**	**SiO_2-PEG**	**D ($\times 10^{-10}$ m^2/s)**
pH = 6	2.49	pH = 7	D1 = 3.1 (I1 = 0.98) D2 = 0.16 (I2 = 0.02)
pH = 9	2.32		
pH = 10.5	2.64		
pH = 12	2.71		

These results tend thus to show that a reaction time of 4h for the grafting of organic molecules on the silica NP surface is not sufficient, so that the grafting was then performed with a reaction time of 24 h.

3.1.2. NMR Analysis of the Silica Nanoparticles Grafted with PEG and with La-p-NH_2-Bn-DTPA Synthesized with a Reaction Time of 24 h

A reaction time of 24 h was first applied for the grafting of PEG on the NP surface and as the NMR characterization was sufficient to prove the covalent grafting (data not shown), La-p-NH_2-Bn-DTPA was also grafted.

An NMR spectrum was recorded on those silica NP and shows the signals characteristic of PEG and of the La-complex (Figure S3). However, as seen in the previous part, this does not prove at all the covalent grafting of PEG and of the La-complex. A DOSY spectrum was thus recorded with a sufficiently long diffusion time of 600 ms (Figure 3). One diffusion coefficient of 6.68 $\times$ 10^{-11} m^2/s was obtained for all the peaks of PEG and La-complex, which tends to prove the covalent grafting of PEG and of the La-complex on the nanoparticle surface.

A quantitative NMR spectrum recorded with an external reference (TSP, see Section 2) allows for the estimation that more or less 75% of the carboxylate groups at the nanoparticle surface are functionalized with PEG and the La-complex: around 7% are functionalized with PEG whereas 68% are functionalized with the La-complex, which means that the La-complex is approximately 10 times more present than PEG at the nanoparticle surface (Figure S4). This can be explained by the synthesis protocol (see Section 2), where the La-complex is first allowed to react for 24 h, followed by PEG.

Interestingly, NMR allows also the witnessing of the degradation of the NP after several months. The same characterization was indeed performed on the silica NP grafted with PEG stored at 4 °C after six months and the results clearly show a starting dissolution of the silica NP, whereas the solution was still homogenous according to both the naked eye and the dynamic light scattering measurements (Figure S5). First, the 1D NMR spectrum clearly shows the doubling of the peaks corresponding to CETS in comparison with the spectrum recorded on the fresh NP (Figure 4), which tends to evidence a destabilization of the NP. Secondly, a further analysis of these peaks with DOSY shows that one has still the same diffusion coefficient than the one measured on the fresh NP, whereas the other has a higher diffusion coefficient, typical of rapid diffusing molecules of small size (Figure 5). This proves definitively that the silica NP are starting to dissolve in the solution, with the CETS at the surface which is progressively leaking from the NP. This phenomenon was already described in the literature [42–44] and is here clearly evidenced by NMR.

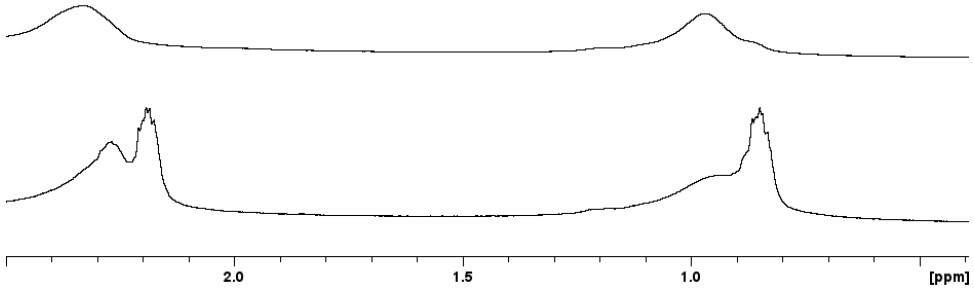


Figure 4. 1D NMR spectra recorded with the sequence noesypr1d on water solutions prepared with 10% D_2O of the silica NP grafted with PEG: above spectrum: spectrum recorded on fresh NP; bottom spectrum: spectrum recorded after 6 months.

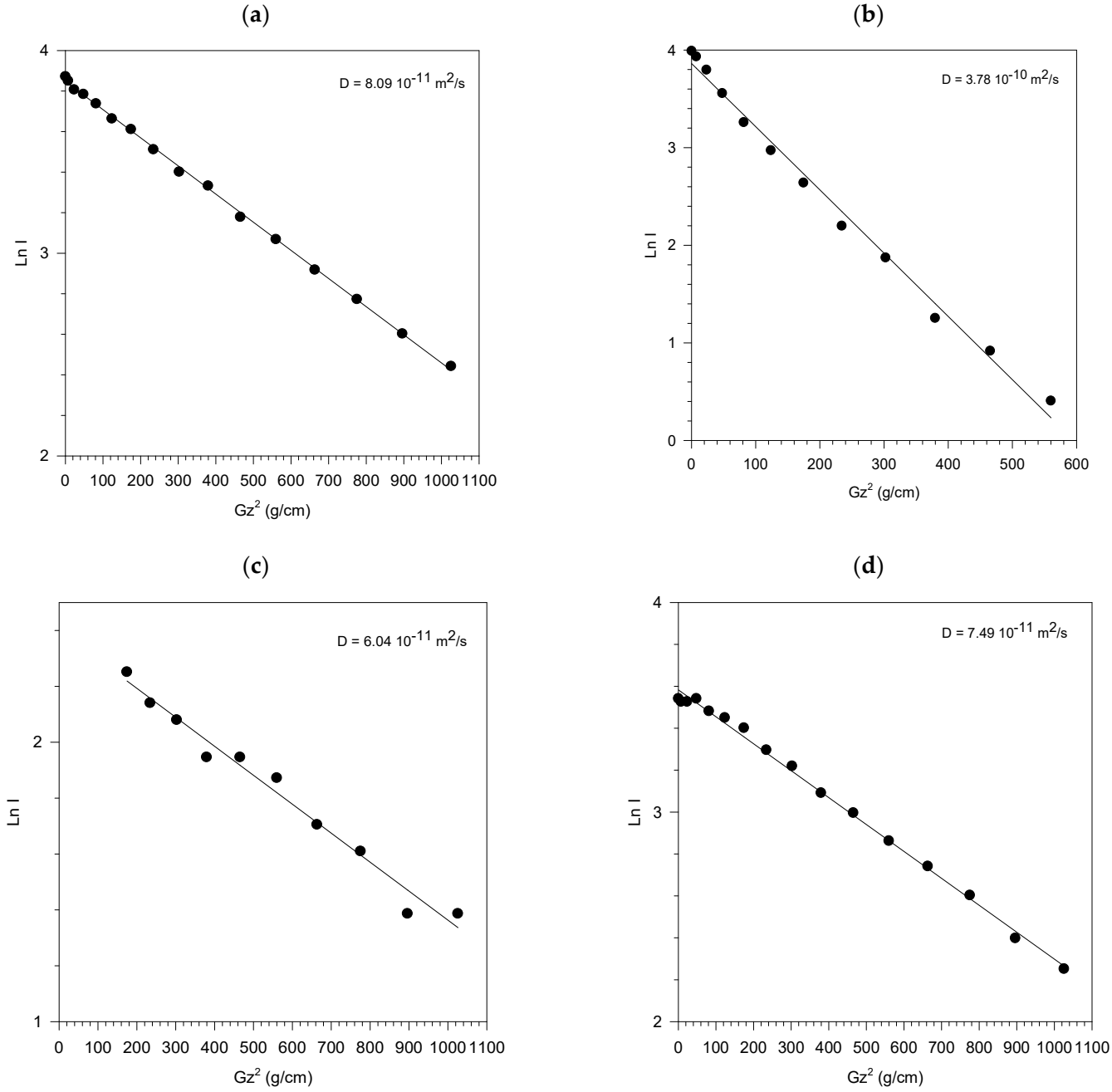


Figure 4. *Cont.*

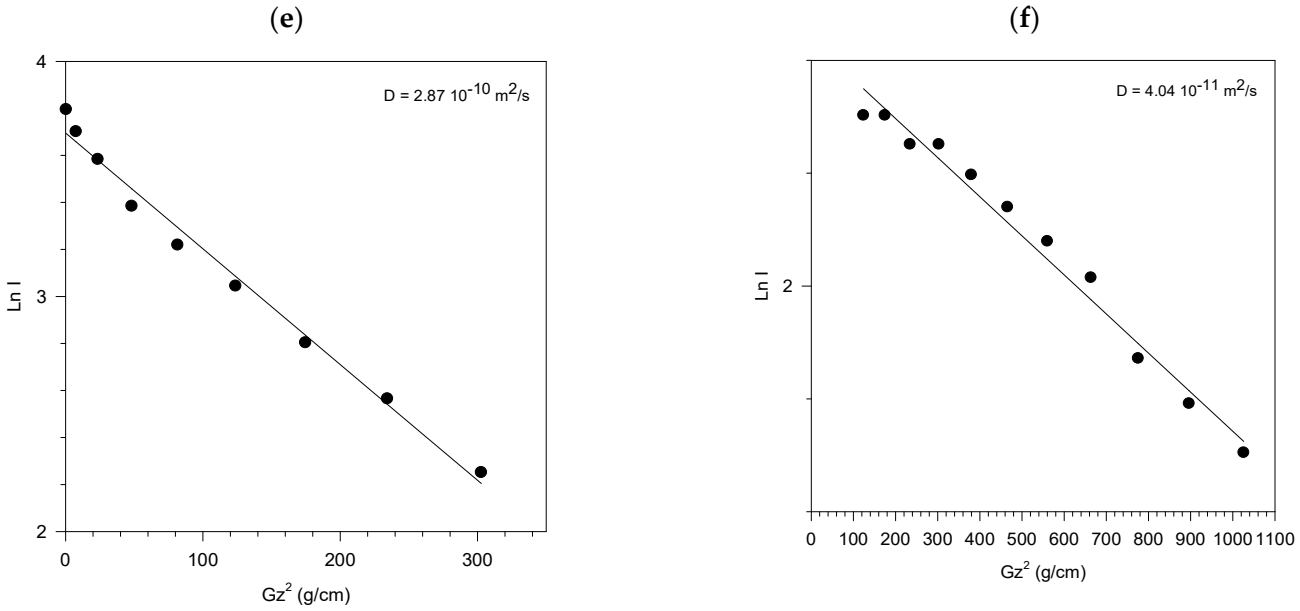


Figure 5. Diffusion curves extracted from the DOSY on CETS peaks. (**a**) CETS peak at 0.9 ppm: fresh NP. (**b**) CETS peak at 0.9 ppm: NP after 6 months (right peak). (**c**) CETS peak at 0.9 ppm: NP after 6 months (left peak). (**d**) CETS peak at 2.3 ppm: fresh NP. (**e**) CETS peak at 2.3 ppm: NP after 6 months (right peak). (**f**) CETS peak at 2.3 ppm: NP after 6 months (left peak).

This first study on silica NP allows for the demonstration of the necessity of a 24 h coupling reaction to efficiently graft organic molecules at the surface, and also shows the starting dissolution of the NP after several months, whereas the solution still appears homogeneous according to dynamic light scattering measurements.

3.2. Bismuth Nanoparticles

3.2.1. Nanoparticles Stabilized with Citrate

A 1D NMR spectrum was recorded on the bismuth NP suspension stabilized with citrate and compared to the spectrum of citrate (Figure 6). These spectra clearly evidence the presence of citrate in the NP suspension, as well as other small peaks which can be attributed to gluconic acid (signals between 3.4 and 4.2 ppm) and isopropanol (signals at 1.2 ppm and between 3.9 and 4 ppm) (Figure S6). The presence of isopropanol can be justified by its use in the rinsing protocol of the HPLC pump, controlling the continuous flow device.

To determine if the citrate is interacting strongly with the NP surface, DOSY spectra were recorded on the NP solution and on citrate for comparison. A diffusion coefficient of 4.6×10^{-10} m^2/s was obtained for citrate in the NP suspension, whereas its diffusion coefficient in water is equal to 5.25×10^{-10} m^2/s. This difference can primarily be explained by the viscosity difference between the two solutions, meaning that citrate does not interact or interacts very weakly with the NP surface. Surprisingly, a biexponential diffusion behaviour was observed for the signal at 1.2 ppm belonging to isopropanol (Figure 7), and two diffusion coefficients can thus be extracted. The first one ($D_1 = 7.7 \times 10^{-10}$ m^2/s) is compatible with free isopropanol, whereas the second one ($D_2 = 1.0 \times 10^{-11}$ m^2/s) is compatible with isopropanol interacting strongly with NP. This result could mean that the NP are mainly stabilized by isopropanol and not only by citrate, and that citrate is not a ligand with a high affinity for the bismuth NP surface.

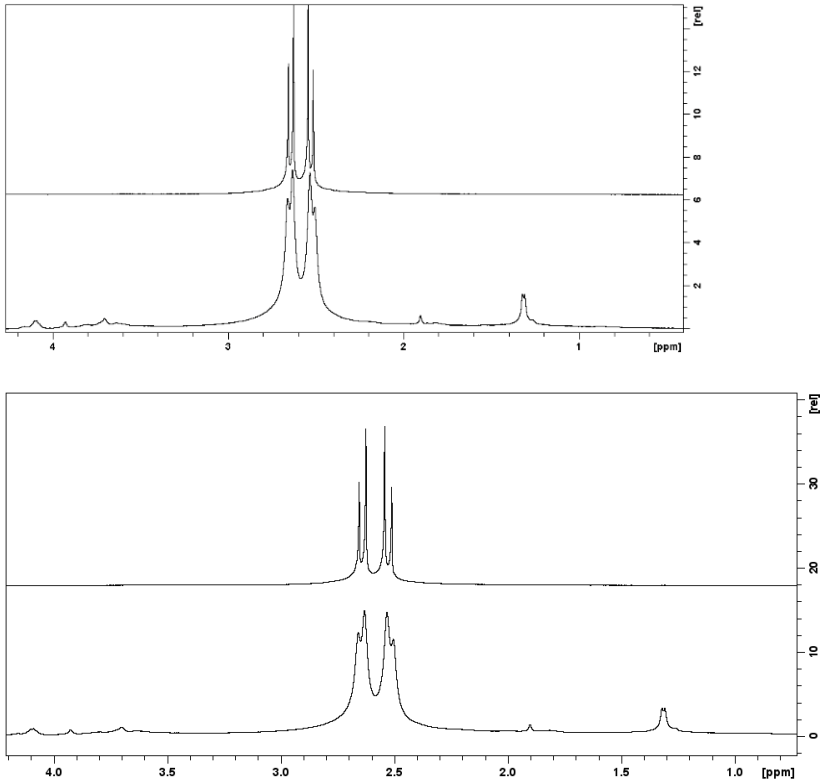


Figure 6. Comparison between 1D NMR spectra recorded with the sequence noesypr1d on water solutions prepared with 10% D_2O of the bismuth NP stabilized with citrate (bottom spectrum) and of citrate (above spectrum).

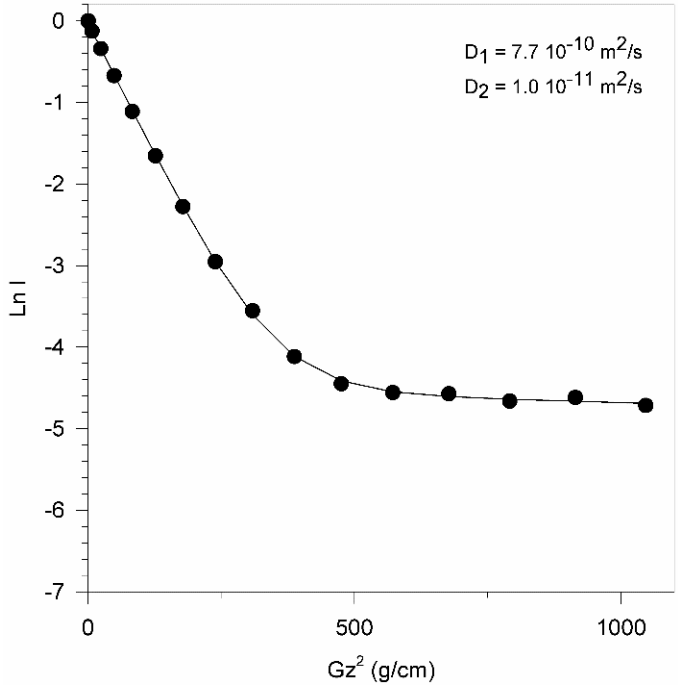


Figure 7. Biexponential diffusion curve extracted from the DOSY experiment recorded on the bismuth NP solution for the signal at 1.2 ppm belonging to isopropanol.

3.2.2. Nanoparticles Stabilized with Lipoic Acid Modified with PEG

The same study was performed on NP stabilized with a derivative of lipoic acid (AL-PEG_{750}-OMe). The thiol groups allow the interaction with the NP surface, whereas

the carboxylic acid function was modified with a PEG chain of molecular weight 750 to further stabilize the NP, provide water solubility and assure a long circulating time in case of in vivo injections. The 1D NMR spectrum of this NP suspension clearly shows all the signals of the ligand (Figure S7) and the DOSY measurement performed on the suspension allows the extraction of the diffusion coefficients on each of those signals. Quite logically, the same behaviour was observed for all peaks of the ligand and the diffusion appears again biexponential, i.e., characterized by two diffusion coefficients. The first one ($D_1 = 2.4 \times 10^{-10}$ m^2/s) is compatible with the free ligand, whereas the second one ($D_2 = 5.45 \times 10^{-11}$ m^2/s) is compatible with the ligand interacting strongly with the surface of NP. This means that part of the ligand is interacting with the NP surface to stabilize them and we can reasonably suppose that the free ligand corresponds to the oxidized form of lipoic acid, whereas the bound form corresponds to its reduced form (Figure 8), via an oxydo-reduction mechanism at the surface. A further analysis of the biexponential curves shows that about 25% of the molecules are diffusing slowly, whereas the other 75% are diffusing as a free ligand.

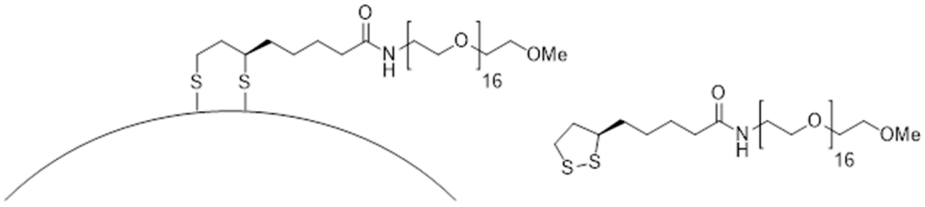


Figure 8. Hypothetic scheme of the grafting of sodium lipoate at the surface of bismuth NP.

In conclusion, this study on bismuth NP has demonstrated that citrate is not an appropriate ligand, whereas lipoic acid, thanks to its thiol groups, is able to interact strongly with the surface to stabilize the NP. This coating agent, which is unusual for metallic bismuth NP but well described for gold NP [45], will offer new prospects for functionalizing stabilized bismuth NP.

4. Conclusions

These two studies illustrate the power of the NMR tools to thoroughly characterize the surface of diamagnetic NP. In particular, DOSY experiments are very useful for these types of studies. However, special attention has to be paid to the diffusion time (Δ) used during the measurements, since we have shown that a too short diffusing time does not allow to evidence the biexponential behaviour due to the presence of a rapid diffusing species and a lower quantity of a slow diffusing species. Some important information could thus be missed.

Supplementary Materials: The following are available online at https://www.mdpi.com/article/10.3390/applnano2040024/s1, Figure S1: COSY spectra of silica NPs grafted with PEG at different pH: (a) pH = 6; (b) pH = 9; (c) pH = 10.5; (d) pH = 12, Figure S2: Diffusion curves extracted from DOSY measurements performed on silica NPs grafted with PEG: (a) signal at 3.6 ppm (b) signal at 3.1 ppm corresponding to the methylene next to the amine function, Figure S3: 1D NMR spectrum recorded with the noesypr1d sequence on a water solution prepared with 10% D_2O of the NPs grafted with PEG and the La-complex, Figure S4: 1D NMR spectrum recorded with the noesypr1d sequence on a water solution prepared with 10% D_2O of the NPs grafted with PEG and the La-complex. An external reference visible at 0 ppm (TSP) was used at a known concentration of 0.8 M, Figure S5: DLS measurements, shown as number distributions, performed on fresh silica NPs grafted with PEG and on the same particles after 6 months, Figure S6: 1D NMR spectra recorded on the bismuth NPs solution stabilized with citrate (bottom spectrum), on gluconic acid (middle spectrum) and on isopropanol (above spectrum), Figure S7: Comparison between 1D NMR spectra recorded with the sequence noesypr1d on water solutions prepared with 10% D_2O of the bismuth NPs stabilized with AL-PEG_{750}-OMe (above spectrum) and of AL-PEG_{750}-OMe (bottom spectrum).

Author Contributions: The manuscript was written through contributions of all authors. Conceptualization, C.H., E.L., C.G., G.H., M.P. and S.L.; methodology, C.H., E.L., C.G., G.H., M.P. and S.L.; formal analysis, C.H., E.L. and G.H.; investigation, C.H., E.L. and G.H.; resources, C.H., E.L. and G.H.; data curation, C.H., E.L. and G.H.; writing—original draft preparation, C.H.; writing—review and editing, C.H., E.L., C.G., G.H., M.P., L.V.E., R.N.M. and S.L.; visualization, C.H., E.L., C.G., G.H., M.P., L.V.E., R.N.M. and S.L.; supervision, M.P. and S.L.; project administration, M.P. and S.L.; funding acquisition, M.P. and S.L. All authors have read and agreed to the published version of the manuscript.

Funding: This research received no external funding.

Institutional Review Board Statement: Not applicable.

Informed Consent Statement: Not applicable.

Acknowledgments: This work was performed with the financial support of ARC, the Walloon Region (Gadolymph, Prother-Wal and Interreg projects), FNRS, and the COST actions. Authors thank the Center for Microscopy and Molecular Imaging (CMMI, supported by European Regional Development Fund and Wallonia). The authors thank the ministerial scholarship for the support of 686 G.H.'s Ph.D. (ED406, Sorbonne University).

Conflicts of Interest: The authors declare no conflict of interest.

References

1. Grumezescu, A.M. (Ed.) *Inorganic Frameworks as Smart Nanomedicines*; Elsevier: Amsterdam, The Netherlands, 2018. [CrossRef]
2. Dumas, C.; Meledandri, C.J. Insights into the Partitioning Behavior of Secondary Surfactants in a Microemulsion-Based Synthesis of Metal Nanoparticles: A DLS and 2D NMR Spectroscopic Investigation. *Langmuir* **2015**, *31*, 7193–7203. [CrossRef]
3. Sarker, M.; Fraser, R.E.; Lumsden, M.D.; Anderson, D.J.; Rainey, J.K. Characterization of Variant Soft Nanoparticle Structure and Morphology in Solution by NMR Spectroscopy. *J. Phys. Chem. C* **2015**, *119*, 7461–7471. [CrossRef]
4. Henoumont, C.; Laurent, S.; Muller, R.N.; Vander Elst, L. HR-MAS NMR spectroscopy: An innovative tool for the characterization of iron oxide nanoparticles tracers for molecular imaging. *Anal. Chem.* **2015**, *87*, 1701–1710. [CrossRef] [PubMed]
5. Van Zijl, P.C.M.; Sehgal, A.A. Proton chemical exchange saturation transfer (CEST) MRS and MRI. *eMagRes* **2016**, *5*, 1307–1332.
6. Ferrauto, G.; Delli Castelli, D.; Di Gregorio, E.; Terreno, E.; Aime, S. LipoCEST and cellCEST imaging agents: Opportunities and challenges. *WIREs Nanomed. Nanobiotechnol.* **2016**, *8*, 602–618. [CrossRef]
7. McMahon, M.T.; Gilad, A.A. Cellular and Molecular Imaging Using Chemical Exchange Saturation Transfer. *Top. Magn. Reson. Imaging* **2016**, *25*, 197–204. [CrossRef] [PubMed]
8. Geraldes, C.F.G.C.; Laurent, S. Classification and basic properties of contrast agents for magnetic resonance imaging. *Contrast Media Mol. Imaging* **2009**, *4*, 1–23. [CrossRef] [PubMed]
9. Laurent, S.; Henoumont, C.; Stanicki, D.; Boutry, S.; Lipani, E.; Belaid, S.; Muller, R.N.; Vander Elst, L. MRI Contrast Agents, from molecules to particles. In *SpringerBriefs in Applied Sciences and Technology*; Springer Nature: Singapore, 2017.
10. Laurent, S.; Henoumont, C.; Vander Elst, L.; Muller, R.N. Synthesis and Physicochemical Characterisation of Gd-DTPA Derivatives as Contrast Agents for MRI. *Eur. J. Inorg. Chem.* **2012**, *2012*, 1889–1915. [CrossRef]
11. Bonnet, C.S.; Toth, E. Molecular magnetic resonance imaging probes based on Ln^{3+} complexes. *Adv. Inorg. Chem.* **2016**, *68*, 43–96.
12. Aime, S.; Botta, M.; Terreno, E. Gd(III)-based contrast agents for MRI. *Adv. Inorg. Chem.* **2005**, *57*, 173–237.
13. Laurent, S.; Forge, D.; Port, M.; Roch, A.; Robic, C.; Vander Elst, L.; Muller, R.N. Magnetic iron oxide nanoparticles: Synthesis, stabilization, vectorization, physicochemical characterizations, and biological applications. *Chem Rev.* **2008**, *108*, 2064–2110, Erratum in *Chem. Rev.* **2010**, *110*, 2574. [CrossRef]
14. Mathieu, P.; Coppel, Y.; Respaud, M.; Thi Quyen, N.; Boutry, S.; Laurent, S.; Stanicki, D.; Henoumont, C.; Novio, F.; Lorenzo, J.; et al. Silica Coated Iron/Iron Oxide Nanoparticles as a Nano-Platform for T_2 Weighted Magnetic Resonance Imaging. *Molecules* **2019**, *24*, 4629. [CrossRef]
15. Washner, J.; Gale, E.M.; Rodriguez-Rodriguez, A.; Caravan, P. Chemistry of MRI Contrast Agents: Current Challenges and New Frontiers. *Chem. Rev.* **2019**, *119*, 957–1057. [CrossRef]
16. Devreux, M.; Henoumont, C.; Dioury, F.; Stanicki, D.; Boutry, S.; Larbanoix, L.; Ferroud, C.; Muller, R.N.; Laurent, S. Bimodal Probe for Magnetic Resonance Imaging and Photoacoustic Imaging Based on a PCTA-Derived Gadolinium(III) Complex and ZW800–1. *Eur. J. Inorg. Chem.* **2019**, *29*, 3354–3365. [CrossRef]
17. Botta, M.; Tei, L. Relaxivity Enhancement in Macromolecular and Nanosized Gd^{III}-Based MRI Contrast Agents. *Eur. J. Inorg. Chem.* **2012**, *12*, 1945–1960. [CrossRef]
18. Mertz, D.; Affolter-Zbaraszczuk, C.; Barthès, J.; Cui, J.; Caruso, F.; Baumert, T.F.; Voegel, J.-C.; Ogier, J.; Meyer, F. Templated assembly of albumin-based nanoparticles for simultaneous gene silencing and magnetic resonance imaging. *Nanoscale* **2014**, *6*, 11676–11680. [CrossRef]

19. Chen, W.; Cormode, D.P.; Vengrenyuk, Y.; Herranz, B.; Feig, J.E.; Klink, A.; Mulder, W.J.M.; Fisher, E.A.; Fayad, Z.A. Collagen-specific peptide conjugated HDL nanoparticles as MRI contrast agent to evaluate compositional changes in atherosclerotic plaque regression. *JACC Cardiovasc. Imaging* **2013**, *6*, 373–384. [CrossRef]
20. Smith, C.E.; Shkumatov, A.; Withers, S.G.; Yang, B.; Glockner, J.F.; Misra, S.; Roy, E.J.; Wong, C.-H.; Zimmerman, S.C.; Kong, H. A Polymeric Fastener Can Easily Functionalize Liposome Surfaces with Gadolinium for Enhanced Magnetic Resonance Imaging. *ACS Nano* **2013**, *7*, 9599–9610. [CrossRef]
21. Moghaddam, M.J.; De Campo, L.; Hirabayashi, M.; Bean, P.A.; Waddington, L.J.; Scoble, J.A.; Coia, G.; Drummond, C.J. Gadolinium-DTPA amphiphile nanoassemblies: Agents for magnetic resonance imaging and neutron capture therapy. *Biomater. Sci.* **2014**, *2*, 924–935. [CrossRef]
22. Ndiaye, M.; Malytskyi, V.; Vangijzegem, T.; Sauvage, F.; Wels, M.; Cadiou, C.; Moreau, J.; Henoumont, C.; Muller, R.N.; Harakat, D.; et al. Comparison of MRI Properties between Multimeric DOTAGA and DO3A Gadolinium-Dendron Conjugates. *Inorg. Chem.* **2019**, *58*, 12798–12808. [CrossRef] [PubMed]
23. Granato, L.; Longo, D.; Boutry, S.; Vander Elst, L.; Henoumont, C.; Aime, S.; Muller, R.N.; Laurent, S. Synthesis and Relaxometric Characterization of New Poly[N,N-bis(3-aminopropyl)glycine] (PAPGly) Dendrons Gd-Based Contrast Agents and Their in Vivo Study by Using the Dynamic Contrast-Enhanced MRI Technique at Low Field (1 T). *Chem. Biodivers.* **2019**, *16*, e1900322. [CrossRef] [PubMed]
24. Li, Y.; Duong, H.T.T.; Laurent, S.; Macmillan, A.; Whan, R.M.; Vander Elst, L.; Muller, R.N.; Hu, J.; Lowe, A.; Boyer, C.; et al. Nanoparticles based on star polymers as theranostic vectors: Endosomal-triggered drug release combined with MRI sensitivity. *Adv. Healthc. Mater.* **2015**, *4*, 148–156. [CrossRef] [PubMed]
25. Lim, C.-K.; Singh, A.; Heo, J.; Kim, D.; Lee, K.E.; Jeon, H.; Koh, J.; Kwon, I.-C.; Kim, S. Gadolinium-coordinated elastic nanogels for in vivo tumor targeting and imaging. *Biomaterials* **2013**, *34*, 6846–6852. [CrossRef] [PubMed]
26. Abdukayum, A.; Yang, C.-X.; Zhao, Q.; Chen, J.-T.; Dong, L.-X.; Yan, X.-P. Gadolinium Complexes Functionalized Persistent Luminescent Nanoparticles as a Multimodal Probe for Near-Infrared Luminescence and Magnetic Resonance Imaging in Vivo. *Anal. Chem.* **2014**, *86*, 4096–4101. [CrossRef] [PubMed]
27. Lin, B.; Yao, X.; Zhu, Y.; Shen, J.; Yang, X.; Li, C. Multifunctional gadolinium-labeled silica-coated core/shell quantum dots for magnetic resonance and fluorescence imaging of cancer cells. *RSC Adv.* **2014**, *4*, 20641–20648. [CrossRef]
28. Lipani, E.; Laurent, S.; Surin, M.; Vander Elst, L.; Leclère, P.; Muller, R.N. High-Relaxivity and Luminescent Silica Nanoparticles as Multimodal Agents for Molecular Imaging. *Langmuir* **2013**, *29*, 3419–3427. [CrossRef] [PubMed]
29. Luo, Y.; Hossain, M.; Wang, C.; Qiao, Y.; An, J.J.; Ma, L.; Su, M. Targeted nanoparticles for enhanced X-ray radiation killing of multidrug-resistant bacteria. *Nanoscale* **2013**, *5*, 687–694. [CrossRef] [PubMed]
30. Hossain, M.; Su, M. Nanoparticle location and material dependent dose enhancement in X-ray radiation therapy. *J. Phys. Chem. C Nanomater. Interfaces* **2012**, *116*, 23047–23052. [CrossRef] [PubMed]
31. Deng, J.; Xu, S.; Hu, W.; Xun, X.; Zheng, L.; Su, M. Tumor targeted, stealthy and degradable bismuth nanoparticles for enhanced X-ray radiation therapy of breast cancer. *Biomaterials* **2018**, *154*, 24–33. [CrossRef]
32. Jiao, L.; Li, Q.Q.; Deng, J.; Okosi, N.; Xia, J.; Su, M. The versatile biomedical applications of bismuth-based nanoparticles and composites: Therapeutic, diagnostic, biosensing, and regenerative properties. *Nanoscale* **2018**, *10*, 6751–6757. [CrossRef] [PubMed]
33. Brown, A.L.; Naha, P.C.; Benavides-montes, V.; Litt, H.I.; Goforth, A.M.; Cormode, D.P. Synthesis, X-ray Opacity, and Biological Compatibility of Ultra-High Payload Elemental Bismuth Nanoparticle X-ray Contrast Agents. *Chem. Mater.* **2014**, *26*, 2266–2274. [CrossRef] [PubMed]
34. Chakravarty, S.; Unold, J.; Shuboni-mulligan, D.D.; Blanco-fernandez, B.; Shapiro, E.M. Surface engineering of bismuth nanocrystals to counter dissolution. *Nanoscale* **2016**, *8*, 13217–13222. [CrossRef] [PubMed]
35. Swy, E.R.; Schwartz-Duval, A.S.; Shuboni, D.D.; Latourette, M.T.; Mallet, C.L.; Parys, M.; Cormode, D.P.; Shapiro, E.M. Dual-modality, fluorescent, PLGA encapsulated bismuth nanoparticles for molecular and cellular fluorescence imaging and computed tomography. *Nanoscale* **2014**, *6*, 13104–13112. [CrossRef] [PubMed]
36. Wei, B.; Zhang, X.; Zhang, C.; Jiang, Y.; Fu, Y.Y.; Yu, C.; Sun, S.K.; Yan, X.P. Facile Synthesis of Uniform-Sized Bismuth Nanoparticles for CT Visualization of Gastrointestinal Tract in Vivo. *ACS Appl. Mater. Interfaces* **2016**, *8*, 12720–12726. [CrossRef]
37. Gomez, C.; Hallot, G.; Pastor, A.; Laurent, S.; Brun, E.; Sicard-Roselli, C.; Port, M. Metallic bismuth nanoparticles: Towards a robust, productive and ultrasound assisted synthesis from batch to flow-continuous chemistry. *Ultrason. Sonochem.* **2019**, *56*, 167–173. [CrossRef] [PubMed]
38. Branca, M.; Corp, K.; Ciuculescu-Pradines, D.; Coppel, Y.; Lecante, P.; Amiens, C. Insights into the chemistry of bismuth nanoparticles. *New J. Chem.* **2017**, *41*, 5960–5966. [CrossRef]
39. Hallot, G.; Cagan, V.; Laurent, S.; Gomez, C.; Port, M. A greener chemistry process using microwaves in continuous flow to synthesize metallic bismuth nanoparticles. *ACS Sustain. Chem. Eng.* **2021**, *9*, 9177–9187. [CrossRef]
40. Johnson Jr, C.S. Diffusion ordered nuclear magnetic resonance spectroscopy: Principles and applications. *Prog. Nucl. Magn. Reson. Spectrosc.* **1999**, *34*, 203–256. [CrossRef]
41. Augé, S.; Amblard-Blondel, B.; Delsuc, M.-A. Investigation of the diffusion measurement using PFG and test of the robustness against experimented conditions and parameters. *J. Chim. Phys.* **1999**, *96*, 1559–1565. [CrossRef]

42. Aureli, F.; D'Amato, M.; De Berardis, B.; Raggi, A.; Chiara Turco, A.; Cubadda, F. Investigating agglomeration and dissolution of silica nanoparticles in aqueous suspensions by dynamic reaction cell inductively coupled plasma-mass spectrometry in time resolved mode. *J. Anal. At. Spectrom.* **2012**, *27*, 1540–1548. [CrossRef]
43. Fontecave, T.; Sanchez, C.; Azaïs, T.; Boissière, C. Chemical Modification As a Versatile Tool for Tuning Stability of Silica Based Mesoporous Carriers in Biologically Relevant Conditions. *Chem. Mater.* **2012**, *24*, 4326–4336. [CrossRef]
44. Mahon, E.; Hristov, D.R.; Dawson, K.A. Stabilising fluorescent silica nanoparticles against dissolution effects for biological studies. *Chem. Commun.* **2012**, *48*, 7970–7972. [CrossRef] [PubMed]
45. Chen, X.; Wei, M.; Jiang, S.; Förster, S. Two Growth Mechanisms of Thiol-Capped Gold Nanoparticles Controlled by Ligand Chemistry. *Langmuir* **2019**, *35*, 12130–12138. [CrossRef] [PubMed]